



Adsorption of chromium(VI) from saline wastewater using spent tea-supported magnetite nanoparticle

Ali Akbar Babaei^{a,b}, Mehdi Ahmadi^{a,b}, Gholamreza Goudarzi^{a,b}, Nemat Jaafarzadeh^{a,b}, Zeynab Baboli^{c,*}

^aEnvironmental Technologies Research Center, Ahvaz Jundishapur University of Medical Sciences, Ahvaz, Iran, Tel. +98 61 33738269; emails: babaei-a@ajums.ac.ir (A.A. Babaei), ahmadi241@gmail.com (M. Ahmadi), rgoodarzy@gmail.com (G. Goudarzi), n.jaafarzade@yahoo.com (N. Jaafarzadeh)

^bDepartment of Environmental Health Engineering, School of Public Health, Ahvaz Jundishapur University of Medical Sciences, Ahvaz, Iran

^cBehbahan Faculty of Medical Sciences, Department of Environmental Health Engineering, School of Public Health, Behbahan, Iran, Tel. +98 61 52887201; Fax: +98 61 52887232; email: baboliz87@gmail.com

Received 4 October 2014; Accepted 4 May 2015

ABSTRACT

Spent tea-supported magnetite (ST/Mag) nanoparticles were synthesized as an adsorbent for the removal of hexavalent chromium [Cr(VI)] from saline wastewater. Prepared ST/Mag adsorbent was characterized using X-ray diffraction, scanning electron microscopy, and Fourier transform infrared spectroscopy. Various factors affecting the uptake behavior such as pH, contact time, initial concentration of metal ions, adsorbent dose, coexisting ions, and desorption behavior were studied using batch tests. The results revealed that adsorption of Cr(VI) was highly pH dependent and the kinetics of the adsorption followed by the Avrami fractional-order and pseudo-second-order kinetic models. The results showed that the adsorption isotherms were more accurately represented by Langmuir and Liu isotherm models with a sorption capacity of 30.0 mg g⁻¹. Adsorption experiments with co-ions indicated that the adsorptive removal of Cr(VI) ions was slightly decreased. Desorption studies using alkaline eluents showed maximum recovery of ST/Mag and only 10% decrease occurring in maximum adsorption capacity after five cycles. The ST/Mag nanoparticles proved to be a very prospective adsorbent for Cr(VI) uptake from industrial high-TDS effluents.

Keywords: Chromium(VI); Spent tea-supported magnetite nanoparticles; Adsorption; Saline wastewater

1. Introduction

In recent years, nanoscale iron oxides have increasingly been used for environmental remediation purposes. Among the iron oxides, magnetite (Fe₃O₄) is

a reliable choice for remediation applications owing to its biocompatibility and suitable magnetic properties [1]. Magnetic separation technology is a new methodology that has been used as a simple, fast, efficient, and economical method for separation and preconcentration of environmental contaminants.

*Corresponding author.

Other advantages of this method are the large active surface area and the high adsorption capacity as well as the ability to process a solution containing suspended solids and producing less secondary waste [2,3]. In addition, magnetite can easily be separated by an external magnetic field which is especially useful for the recovery or reuse of magnetite nanoparticles [4]. The disadvantage of using these nanoparticles, however, is their aggregation in aqueous media, which introduces a challenge for work with nanomaterials. This property decreases the effective surface area of the particles and thus reduces their adsorption capacity [4,5]. Agglomeration is also occurring frequently as a result of the encounter between colloidal particles dispersed in the liquid media, and the stability of the dispersion is determined by the interaction between the particles during this encounter. To promote a stable dispersion, short-range repulsive forces are required to keep each particle discrete and prevent it from amassing as larger and faster settling agglomerates [6]. A variety of methods such as surfactant [4,7,8], polymer matrix [9–11], montmorillonite [12], diatomite [13], starch [14], porous silica [15], sepiolite [16], and zeolites [17] have been developed to prevent the co-aggregation and to tailor the size of the nanoparticles.

In this regard, spent tea, which is a kind of natural and readily available household, agricultural, and industrial residue, has been recognized as a non-conventional, low-cost, and efficient biosorbent and also a rich source of environmental friendly hydrocarbons [18]. It has also been found effective for stabilizing magnetite nanoparticles [19]. Recently, a large number of publications have explored the adsorption of organic and inorganic contaminants such as Ni(II) ions [20], Cu and Pb ions [21], chromium(VI) [22], Pb(II) ions [23], and methylene blue [18] from aqueous solutions using spent tea, yet few researchers have worked on impregnated spent tea for the removal of heavy metal ions [24]. Studies have revealed that pure magnetite nanoparticles have a lower uptake of heavy metals than the modified and/or supported magnetite nanoparticles [25,26]. Therefore, in the present study, spent tea-supported magnetite (ST/Mag) nanoparticles were synthesized and the nanocomposites were further used for the removal of Cr(VI) from synthetic saline wastewater to evaluate their effectiveness in being used as an adsorbent in environmental remediation.

Chromium is one of the most toxic metals that exists in river water, groundwater, and soil as a result of metal finishing, electroplating industries, leather tanning, metallurgy and chrome preparations, alloy steel manufacturing, pigment synthesis, and dyeing industries [2,5]. Discharge wastewater from these

industries contain Cr(III) and Cr(VI) in concentrations ranging from 10 to 250 mg L⁻¹ [2]. Tanneries are among complexes characterized as intensively polluting industrial units which generate widely varying, high-strength saline wastewater containing Cr(VI) [27]. Cr(VI) exists mainly in the ionic forms of chromate and dichromate (anionic) in aqueous systems [28]. The industrial effluent maximum permissible discharge level of Cr(VI) into water bodies is 0.1 mg L⁻¹ [29].

There are many techniques that have been developed for the removal of Cr(VI) from wastewater, including ion-exchange, chemical precipitation, membrane filtration, and electro deposition, to name a few [27]. But these methods suffer from disadvantages such as requiring large excess of chemicals, generating volumetric sludge, and involving high capital investment. They are not only limited for high operational cost but also inefficient in the removal of some heavy metal ions [28,30]. Adsorption is a cost-effective, widely used technique for the removal of metal ions [28]. Very few researches concentrating on the removal of Cr(VI) from saline wastewater have been conducted using ST/Mag nanoparticles for adsorption and reduction.

Consequently, the objective of this study is to assess the feasibility of using ST/Mag nanoparticles for Cr(VI) removal from synthetic saline wastewater. For this purpose, ST/Mag nanoparticles were synthesized and the resulting materials were used in a series of batch experiments to investigate how the experimental conditions (e.g. pH value, initial Cr(VI) concentrations, contact time, adsorbent dose, and the salinity of solution) influenced the removal of Cr(VI) ion from saline wastewater. Different non-linear isotherm models were used to describe adsorption equilibrium of Cr(VI) ions by ST/Mag nanoparticles. Furthermore, the kinetics involved in the adsorption process was evaluated using different non-linear kinetic models.

2. Materials and methods

2.1. Chemicals and materials

All chemicals were of analytical reagent grade or the highest purity available from Merck Company (Germany). Double-distilled water was used throughout the study. Potassium dichromate (K₂Cr₂O₇, 99%) was used for the preparation of stock solutions of chromium. Analytical grade reagents such as ferrous chloride tetrahydrate (FeCl₂·4H₂O, 99%) and sodium hydroxide (NaOH) were used for the synthesis of magnetite. NaCl and Na₂SO₄ were used for the preparation of saline solutions.

2.2. Adsorbent preparation and characterization

Spent tea leaves were obtained from households. Initially, in order to remove impurities, caffeine, tannin, and color, it was washed several times with distilled water and then severally boiled with distilled water at 100°C. Decolorized spent tea leaves were dried at 65°C for 24 h. Dried spent tea leaves were then activated using sulfuric acid (H₂SO₄). Hence, dried spent tea leaves were immersed in H₂SO₄ solution and vigorously agitated followed by washing with distilled water till the neutral pH of filtrate was observed. Acid was used to increase the proportion of active surfaces and to prevent the elution of tannin compounds that would both stain the treated water and greatly increase the chemical oxygen demand. After drying at 105°C, activated spent tea (AST) was crushed and eventually sieved through a range of sieves, with particles only less than 270 mesh size used in accordance with the ASTM method [31]. After sieving, the AST were dried in an oven at 80–85°C for 2 h and then the samples were stored in plastic bags until used for the synthesis of ST/Mag nanoparticles.

The ST/Mag nanoparticles were synthesized using the co-precipitation method through the following steps: first, 50 mL of an aqueous solution of FeCl₂·4H₂O (5.0 g L⁻¹ as Fe) was added dropwise to a 50 mL of 1% (W/V) spent tea solution under continuous shaking. The mixture was shaken for 30 min to allow the formation of a homogeneous spent tea–Fe²⁺ solution. Then, the pH of the solution was increased slowly to 12 by adding of 0.5 M NaOH solution. The reaction mixture was shaken for 1 h [14]. The ST/Mag was prepared via controlled oxidation of a Fe²⁺ ion solution according to the following equation:



The adsorbent then was washed several times with alcohol and then deionized water until its pH became neutral, collected by magnetic separation and dried at 70°C under vacuum for 12 h. All of the prepared samples were kept in a vacuum desiccator before being used for adsorption experiments.

The specific surface area of the ST/Mag was measured by Brunauer–Emmett–Teller (nitrogen adsorption technique, model Quantachrome, 2000, NOVA) [32]. The bulk density of the adsorbent was determined by specific gravity bottles. A potentiometric method was used to determine the point of zero charge (pH_{ZPC}) [33]. A Metrohm model 713 pH meter was used for pH measurements. The parameters of the adsorbent such as moisture content, ash content, organic matter, solubility in water, and solubility in acid were determined

by ASTM [34]. The physicochemical features of the ST/Mag nanoparticles are listed in Table 1.

BRUKER's Vertex 70 infrared spectrometer was used for the Fourier transform infrared spectroscopy (FTIR) analysis. The surface morphology of ST/Mag nanoparticles was analyzed using a Philips XL-20 scanning electron microscopy (SEM) (Philips Co., The Netherlands) equipped with an energy dispersive X-ray analyzer (EDX) (S-3400N). EDX analysis is an analytical technique used to determine the elemental composition or chemical characterization of a sample. X-ray diffraction (XRD X'pert Philips, HOLLAND) analysis was performed to identify the structure and the composition of synthesized ST/Mag.

2.3. Adsorption experiments

Batch experiments were performed to evaluate the removal rate of Cr(VI) in the presence of ST/Mag nanoparticles. The experiments were performed at room temperature (20 ± 1°C) using 100-ml high-density polyethylene bottles. The stock solution of Cr(VI) (1,000 mg L⁻¹) was prepared by K₂Cr₂O₇ and the concentration range of Cr(VI) prepared from the stock solution varied from 5 to 300 mg L⁻¹. The synthetic saline wastewater containing the appropriate amount of Cr(VI) and co-ions were prepared by adding the stock solution of Cr(VI) and dissolving NaCl and Na₂SO₄ in distilled water. In a typical run, 0.25 g of ST/Mag nanoparticles adsorbent was added into 50 ml of Cr(VI) solution over a period of time on a shaker at 350 rpm. After the aqueous phase was separated magnetically, the concentration of Cr(VI) and total Cr in the solution was determined using a spectrophotometer (Dr-5000, Hack Co.) and a flame atomic absorption spectrometer (Analytic Jena, Vario 6, Germany), respectively. The amount of Cr(III) was determined by subtracting the total Cr and Cr(VI).

Table 1
The main physicochemical characteristics of ST/Mag nanoparticles

Parameters	Values
Moisture content (%)	2.49
Ash content (%)	64
Volatile fraction (%)	33.77
Solubility in water (%)	0.12
Solubility in acid (%)	0.5
pH _{ZPC}	5.25
BET surface area (m ² g ⁻¹)	509
Particle size (nm)	10–100
Bulk density (kgm ⁻³)	0.84

In this study, the effect of pH was investigated in the range 2–8 under the initial Cr(VI) concentration of 10 mg L^{-1} and TDS of 0.5%. The initial pH of the solution was adjusted using 0.1 M HCl or 0.1 M NaOH. The effects of the contact time (2–240 min), the initial concentration of Cr(VI) ($5\text{--}300 \text{ mg L}^{-1}$), the adsorbent dosage ($0.1\text{--}11.0 \text{ g L}^{-1}$), and the co-ions ($1.0\text{--}100 \text{ mS cm}^{-1}$ electrical conductivity) were also examined throughout the experiments. Finally, the 0.2 M NaOH and 0.2 M NaOH + 1.0 M NaCl were used for the desorption study.

The removal efficiency (%R) of Cr(VI) and the adsorption capacity (q_e) were obtained by the following equations:

$$\%R = \frac{C_o - C_e}{C_o} \times 100 \quad (2)$$

$$q_e = \frac{(C_o - C_e)V}{m} \quad (3)$$

where q_e (mg/g) is the amount of adsorbed Cr ions onto the unit amount of the adsorbent, and C_o and C_e (mg/L) are the initial and equilibrium Cr ion concentrations, respectively. V (L) is the volume of the solution, and m (g) is the mass of dry adsorbent used.

2.4. Adsorption isotherm and kinetic models

To determine the parameters of the isotherm and kinetic models, the Cr(VI) adsorption data were fitted to the non-linear kinetic and isotherm models using MATLAB[®] 7.11.0 (R2010b) software, with successive interactions calculated by the Levenberg–Marquardt algorithm. Since the unwanted falsification of error distribution occurs, due to data transformation to a linear form, the non-linear method would logically be superior to the linear one in determining the parameters of the isotherm and kinetic models [35].

Determination of the adsorption isotherm and the related parameters is a basic requirement for designing adsorption systems. In addition, the kinetics describes the adsorbate uptake rate which controls the residence time of adsorbate uptake at the adsorbent–solution interface. Therefore, it is important to be able to predict the metallic ion uptake removal rate from aqueous solutions in order to design an appropriate adsorption unit. Moreover, this provides important information for modeling the processes. In this study, adsorption isotherm models (viz., Langmuir, Freundlich, Redlich–Peterson, Temkin, and Liu isotherms) have been used to investigate the adsorption capacity and the equilibrium coefficients for the

adsorption of Cr(VI) by ST/Mag adsorbent [36]. In order to describe the kinetics of Cr(VI) adsorption onto ST/Mag, characteristic constants were determined using pseudo-first-order equation of Lagergren [37], pseudo-second-order equation of Ho [38], Elovich [39], Avrami fractional-order [40], fractional power, and Weber–Morris intraparticle diffusion [41]. The non-linear equations and constants related to the isotherm and the kinetic models are given in Supplementary Table 1.

2.5. Models fitness

To select the most suitable kinetic and isotherm models, it is necessary to evaluate their validity. Here, the validity of kinetic and isotherm models was assessed by such criteria as the determination coefficient (R^2), the adjusted determination coefficient (R^2_{adj}), the sum squared error (SSE), and the root mean square error (RMSE) [4,36,42]. These criteria describe the goodness of fit between the experimental and predicted data. The best model was chosen based on the lowest RMSE and SSE, as well as with R^2 and R^2_{adj} as close as possible to one. R^2 , R^2_{adj} , SSE, and RMSE can be calculated according to Supplementary Table 2.

3. Results and discussion

3.1. Characterization of ST/Mag

To evaluate the presence of Fe_3O_4 , the structure of ST/Mag nanoparticles was characterized by XRD whose diffractogram is shown in Fig. 1. The XRD pattern of the ST/Mag nanoparticles was prepared in the 2θ range of $10\text{--}80^\circ$. There are diffraction peaks in ST/Mag nanoparticles, which are consistent with the standard pattern for crystalline magnetite with spinal structure and with PDF2 card of Fe_3O_4 (JCPDS NO. 088-0315 Fe_3O_4). The main peaks at $2\theta = 21.6^\circ$, 35.4° , 43.1° , 53.4° , 56.9° , 62.5° , and 74.9° for ST/Mag, which were marked, respectively, by their indices (1 1 1), (2 2 0), (3 1 1), (4 0 0), (4 2 2), (5 1 1), and (4 4 0) plane of a cubic spinal structure of the magnetite nanoparticles. The characteristics and purity of the ST/Mag nanoparticles were evident because the XRD peaks of the nanocrystallites matched well with standard Fe_3O_4 and other crystalline phases were not detected (Fig. 1). So, it confirms the presence of Fe_3O_4 particles in structure of ST/Mag composite.

FTIR spectra of ST/Mag and Cr(VI) sorbed onto ST/Mag composite are shown in Fig. 2. Based on FTIR spectrum of ST/Mag nanoparticles, the band at around $570\text{--}590 \text{ cm}^{-1}$ was assigned to Fe–O groups, which

Table 2

Goodness of fit criteria and coefficients of adsorption kinetic models

	Adsorption kinetic models	Parameters (unit)	Values	R ² adj	RMSE	SSE	
Cr(VI) 10 mg L ⁻¹	Pseudo-first-order (Lagergren)	K_f (min ⁻¹)	0.217	0.940	0.112	0.100	
		q_e (mg g ⁻¹)	1.356				
	Pseudo-second-order (Ho)	k_S (g mg min ⁻¹)	0.244	0.989	0.048	0.018	
		q_e (mg g ⁻¹)	1.437				
	Elovich	α (mg g ⁻¹ min ⁻¹)	9.033	0.967	0.083	0.055	
		β (g mg ⁻¹)	6.103				
	Avrami fractional-order	k_{AV} (min ⁻¹)		0.191	0.997	0.023	0.004
q_e (mg g ⁻¹)			1.435				
n_{AV} (-)		0.501					
Fractional power function	a (mg g ⁻¹ min ^{-b})	0.764	0.947	0.105	0.088		
	b (-)	0.131					
Intraparticle diffusion	k_{id} (mg g ⁻¹ min ^{-0.5})		0.072	0.539	0.310	0.770	
		C (-)	0.645				
Cr(VI) 100 mg L ⁻¹	Pseudo-first-order (Lagergren)	K_f (min ⁻¹)	0.164	0.977	0.710	4.037	
		q_e (mg g ⁻¹)	13.51				
	Pseudo-second-order (Ho)	k_S (g mg min ⁻¹)	0.018	0.998	0.186	0.276	
		q_e (mg g ⁻¹)	14.40				
	Elovich	α (mg g ⁻¹ min ⁻¹)	29.97	0.952	1.022	8.356	
		β (g mg ⁻¹)	0.530				
	Avrami fractional-order	k_{AV} (min ⁻¹)		0.151	0.999	0.165	0.187
			q_e (mg g ⁻¹)	13.92			
		n_{AV} (-)	0.646				
	Fractional power function	a (mg g ⁻¹ min ^{-b})	6.697	0.92	1.325	14.05	
b (-)		0.156					
Intraparticle diffusion	k_{id} (mg g ⁻¹ min ^{-0.5})		0.762	0.583	3.026	73.27	
		C (-)	5.727				

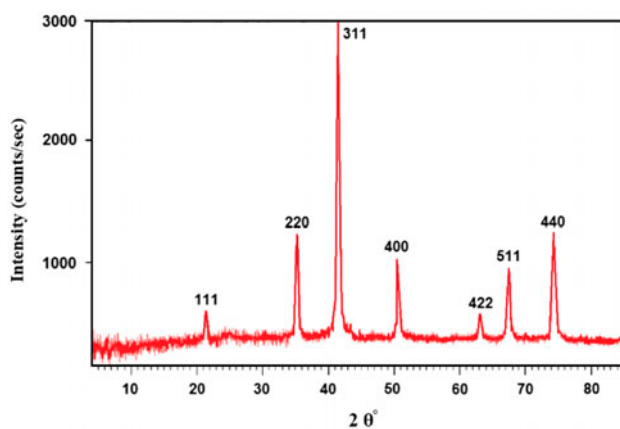


Fig. 1. XRD image of ST/Mag nanoparticles.

confirms the metal–oxygen stretching and indicates the presence of Fe in ST/Mag nanoparticles (see Fig. 2). The trough at 1,055 and 1,640 cm⁻¹ represents the C–O stretching mode corresponding to the carbonyl groups in the alcohol components (phenolic) and C–O stretching mode conjugating with the NH₂ (amide 1 band),

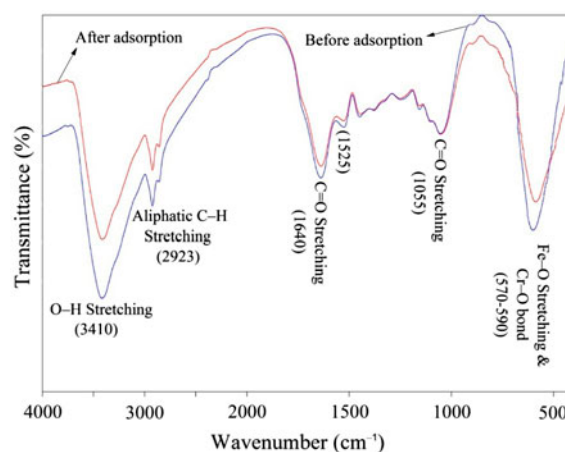


Fig. 2. FTIR spectra of ST/Mag before and after Cr(VI) adsorption.

respectively. The band observed at about 2,923 cm⁻¹ could be assigned to the aliphatic C–H group [19], while peaks appearing at 3,410–3,420 cm⁻¹ in the spectrum (see Fig. 2) are indicative of hydroxyl groups. In the FTIR spectrum of Cr(VI)-sorbed ST/Mag compos-

ite, the broadening of band at $3,420\text{ cm}^{-1}$ in the FTIR spectra of Cr(VI)-sorbed ST/Mag composite illustrates the electrostatic attraction between the HCrO_4^- ions and the ST/Mag. The shiftings in absorption frequencies at 588 cm^{-1} related to Fe–O groups, absorption frequencies at $2,923\text{ cm}^{-1}$ related to aliphatic C–H group, and absorption frequencies at $3,410\text{ cm}^{-1}$ related to OH groups also indicate the electrostatic attraction [43]. In addition, the absorption band at around $570\text{--}590\text{ cm}^{-1}$ corresponds to the Cr–O bond which indicates the presence of Cr(VI) in the chromium-sorbed ST/Mag [44]. It seems that the mentioned functional groups influence the Cr(VI) adsorption on ST/Mag nanoparticles.

The SEM was used to study the surface characteristics and the morphology of the adsorbent. The SEM micrograph of ST/Mag is shown in Fig. 3(a). According to the SEM observation (Fig. 3(a)), the synthesized ST/Mag nanoparticles appear as spherical shape with size in the range 10–100 nm and their

mean sizes are 45 nm. The nanoparticles are aggregated, which resulted in a rough surface and porous structure. Therefore, spherical ST/Mag is at the nanoscale and good to achieve adsorption.

Fig. 3(b) and (c) shows the EDX spectra of ST/Mag adsorbents before and after loaded with Cr(VI), respectively. The EDX spectrum of ST/Mag before interacting with Cr(VI) ions revealed carbon, oxygen, and iron as major components, with Al and Ca representing minor and trace components. Comparing the spectra of the ST/Mag loaded with Cr(VI) with that of unloaded one, the chromium peak could be observed (Fig. 3(c)), which confirmed the chromium adsorption onto the ST/Mag composite.

3.2. Effect of pH

Adsorption studies indicated that pH plays an important role in the adsorption process. To investi-

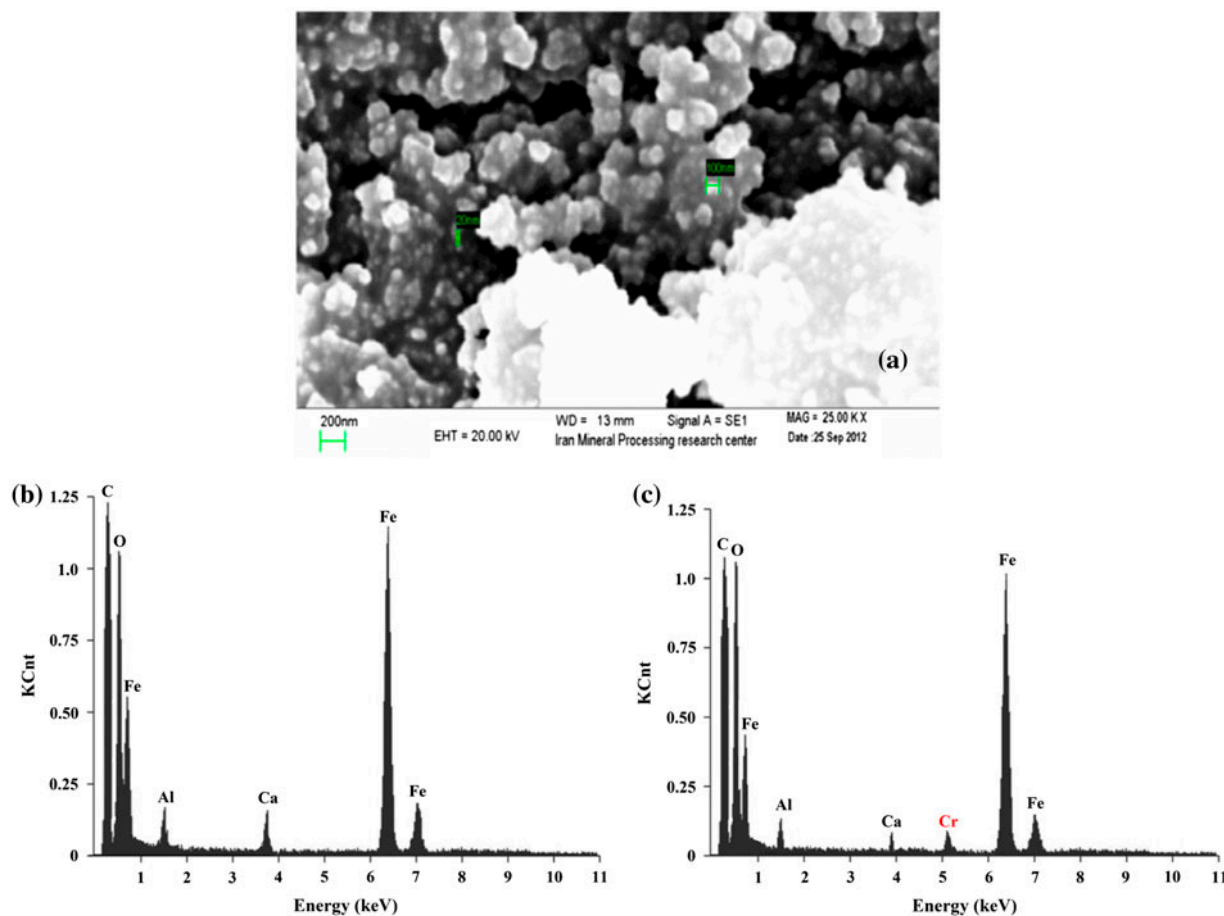


Fig. 3. (a) SEM micrograph of ST/Mag nanoparticles and EDX spectra of the magnetic adsorbents, (b) ST/Mag, and (c) ST/Mag loaded with Cr(VI).

gate the effects of pH on the adsorption of Cr(VI) onto ST/Mag, the initial pH values were adjusted to the range of 2.0–8.0. The initial Cr(VI) and salt concentrations were set at 10 mg L^{-1} and 0.5%, respectively, and the contact time was 120 min. Fig. 4 shows that the uptake of chromium(VI) by spent tea–magnetite is highly pH dependent and that the efficiency of Cr(VI) uptake by ST/Mag decreases as a result of increasing the solution's pH. The maximum removal efficiency (92.8%) of Cr(VI) by ST/Mag nanoparticles was found at pH 2.0. These results are confirmed in other reports as well [3,4,25,45,46]. At first, it may be attributed to affinity of the adsorbent for the different anion species of Cr(VI), namely $\text{Cr}_2\text{O}_7^{2-}$, HCrO_4^- , CrO_4^{2-} , $\text{Cr}_3\text{O}_{10}^{2-}$, and $\text{Cr}_4\text{O}_{13}^{2-}$ coexisting at acidic pH conditions [47]. In the acidic pH range of 2–3, the HCrO_4^- is the most predominant species of Cr(VI), which is favorably adsorbed because of the low adsorption free energy [45]. Moreover, due to the excess amount of H^+ ions within the medium at the acidic pH, the active sites on the adsorbent are positively charged. This causes a strong attraction between these sites as well as a negative charge of different anion species of Cr(VI), especially the HCrO_4^- ions [48]. On the other hand, the surface of ST/Mag has a net positive ($-\text{OH}^{+2}$) [28], a neutral ($-\text{OH}$), and a negative ($-\text{O}^-$) charge at $\text{pH} < \text{pH}_{\text{ZPC}}$, $\text{pH} = \text{pH}_{\text{ZPC}}$, and $\text{pH} > \text{pH}_{\text{ZPC}}$, respectively. Thus, Cr(VI) ions (HCrO_4^- and CrO_4^{2-}) can easily be adsorbed to the surface of magnetite at pH values lower than the pH_{ZPC} [49]. As a result, an increase in pH value will make the ST/Mag surfaces less positively charged, greatly weakening the electrostatic attraction between ST/Mag nanoparticles and negatively charged Cr(VI) anions. In addition, the

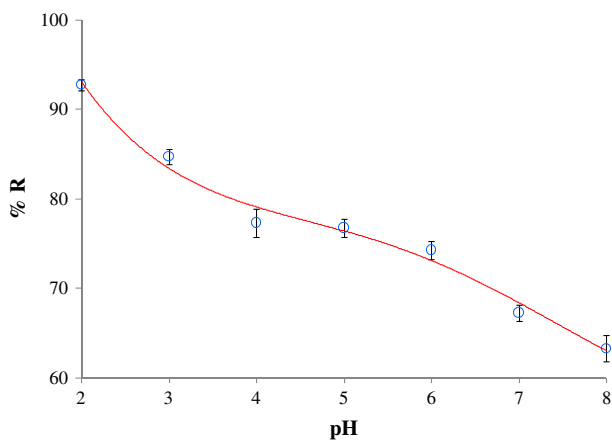


Fig. 4. The effect of pH on Cr(VI) adsorption by ST/Mag nanoparticles (conditions: C_o 10 mg L^{-1} , contact time 120 min, adsorbent dose 5 g L^{-1} , TDS $5,000 \text{ mg L}^{-1}$, and $T = 20 \pm 1^\circ\text{C}$).

significant decrease in the Cr(VI) uptake with the increase in pH values is due to the higher concentration of OH^- ions present in the reaction mixture, which compete with Cr(VI) anions to occupy the adsorption sites and thus reduce the removal efficiency of ST/Mag nanoparticles.

3.3. Effect of adsorbent dose

The adsorbent dose parameter has a pronounced effect on the removal of adsorbate species from aqueous solutions. In the present study, the effect of different ST/Mag dosages on Cr(VI) removal from aqueous solutions was investigated. As shown in Fig. 5, the removal efficiency increased from 10.1 to 99.7% upon increasing the adsorbent dose from 0.10 to 11.0 g L^{-1} . Maximum removal of Cr(VI) was achieved by ST/Mag in the optimum dose of 6 g L^{-1} , but afterward, the Cr(VI) removal efficiency was almost constant. This result was expected because as the adsorbent dose increases, the number of adsorbent particles and active sites increases and thus more Cr(VI) is attached to their surfaces. According to Babaei et al. [4] and Wang et al. [50], increase in the adsorbent dose leads to an increase in the removal efficiency of Cr(VI) using different adsorbents.

3.4. Effect of contact time and adsorption kinetics

The adsorption of Cr(VI) by ST/Mag nanoparticles as a function of time at the initial Cr(VI) concentrations of 10 and 100 mg L^{-1} is displayed in Fig. 6. The unit of adsorption of Cr(VI) increased from 1.44 to

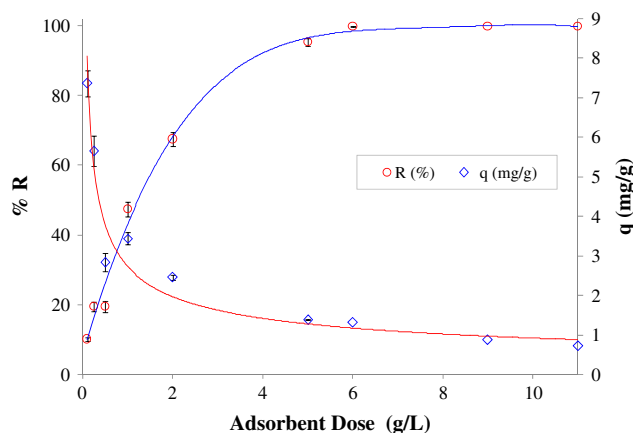


Fig. 5. Effect of adsorbent dose on Cr(VI) removal by ST/Mag (conditions: pH 2, C_o 10 mg L^{-1} , contact time 120 min, TDS $5,000 \text{ mg L}^{-1}$, and $T = 20 \pm 1^\circ\text{C}$).

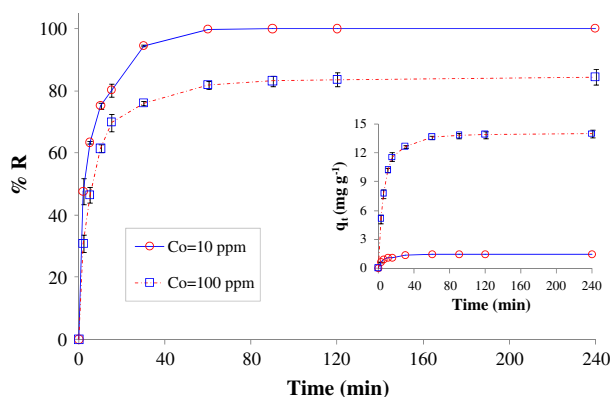


Fig. 6. Effect of contact time on adsorption of Cr(VI) (conditions: pH 2.0, adsorbent dose 6.0 g L^{-1} , TDS $5,000 \text{ mg L}^{-1}$, and $T = 20 \pm 1^\circ \text{C}$).

13.92 mg g^{-1} as the initial Cr(VI) concentration rose from 10 to 100 mg L^{-1} . As shown in Fig. 6, the rate of Cr(VI) uptake was quite fast for the first 30 min, reaching the equilibrium after 60 min for the two values of the initial Cr(VI) concentration studied. At equilibrium state, the removal efficiencies of Cr(VI) with the initial concentrations of 10 and 100 mg L^{-1} were 99.7 and 81.8%, respectively. The higher sorption rate at the initial period (first 30 min) is probably due to the plentiful availability of sorption sites and a large surface area available for the adsorption of the Cr(VI) onto ST/Mag. It may as well be attributed to the external surface adsorption. This indicates that a significant part of adsorption sites of the adsorbent exists in the exterior of ST/Mag nanoparticles and is easily accessible by the Cr(VI) species, thus resulting in a rapid equilibrium. According to Babaei et al. [4] and Yuan et al. [13], adsorption equilibrium was achieved in 1 h in the acidic pH range in the presence of SLS-Mag and montmorillonite-supported magnetite, respectively.

The kinetics of the adsorption process is shown in Fig. 7 was simulated with 99% confidence bounds using non-linear equations of pseudo-first-order of Lagergren, pseudo-second-order of Ho, fractional power, Elovich, Avrami fractional-order, and Weber–Morris intraparticle diffusion kinetic models. The estimated parameters are shown in Table 2. From Table 2 and Fig. 7, it can be seen that the intraparticle diffusion (ID) model has the least fit to the experimental data, which indicates that intraparticle diffusion is not a controlling step during the sorption of Cr(VI) on ST/Mag nanoparticles and that some other mechanisms are involved. Based on the higher value of the adjusted determination coefficient (R^2_{adj}) and the lower values of the SSE and the RMSE, it is found that

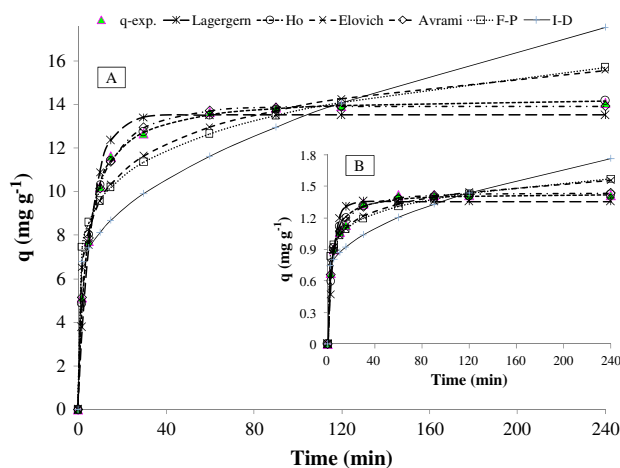


Fig. 7. Non-linear adsorption kinetics of Cr(VI) on ST/Mag nanoparticles: (a) C_0 100 mg L^{-1} and (b) C_0 10 mg L^{-1} (conditions: pH 2.0, adsorbent dose 6 g L^{-1} , TDS 0.5%, and $T = 20 \pm 1^\circ \text{C}$).

Cr(VI) adsorption onto ST/Mag nanoparticles can be best described by the Avrami fractional-order and pseudo-second-order kinetic models for the two values of the initial Cr(VI) concentrations studied. This result indicates that this sorption system is a pseudo-second-order reaction, implying the rate-limiting step may be a chemical sorption involving valency forces through sharing or exchanging electrons between sorbent and sorbate [38].

3.5. Effect of initial Cr(VI) concentration and adsorption isotherm

The initial concentration of contaminants provides an important driving force to overcome all the mass transfer resistance of metal ion between the aqueous and solid phases. Hence, a higher initial concentration of Cr(VI) will increase the adsorption rate [47]. Removal of Cr(VI) by ST/Mag nanoparticles as a function of initial Cr(VI) concentrations at pH 2 is shown in Fig. 8. At equilibrium condition, increasing the initial concentration of Cr(VI) led to a decrease in the removal efficiency of Cr(VI), but the values of q_e increased by increasing the initial concentration of Cr(VI) in the presence of salt. It was clear that the adsorption capacity increased from 1.66 to 26.06 mg g^{-1} with an increase in initial Cr(VI) concentration from 10 to 100 mg L^{-1} until equilibrium was reached. This might be attributed to an increase in the driving force of the concentration gradient with the increase in initial Cr(VI) concentration. On the other hand, Cr(VI) removal efficiency is inversely related to the initial chromium concentrations, due to an

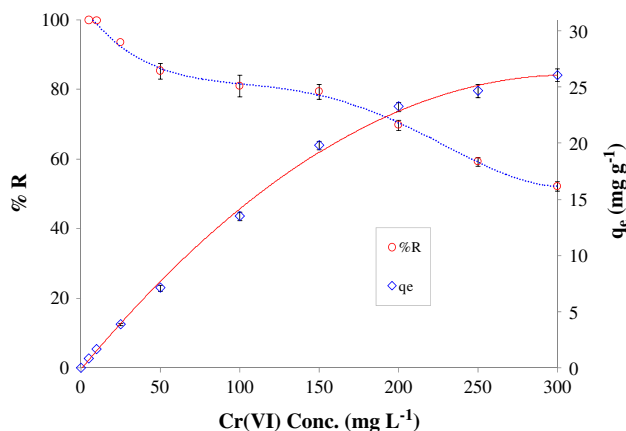


Fig. 8. Initial concentration effect on Cr(VI) removal by ST/Mag (conditions: C_o 10 mg L⁻¹, pH 2, adsorbent dose 6 g L⁻¹, contact time 60 min, TDS 0.5%, and $T = 20 \pm 1$ °C).

increase in the number of ions competing with the increased initial concentration for the available binding sites in the adsorbent. It also has limited active sites that are saturated in higher concentrations.

Analysis of the equilibrium data is important in designing adsorption systems. In this study, experimental data were fitted to five widely used adsorption isotherm models including Langmuir, Freundlich, Redlich–Peterson, Liu, and Temkin employing non-linear equations (see Fig. 9). Parameters of the adsorption equilibrium isotherms of Cr(VI) onto ST/Mag are given in Table 3. Although based on the R^2_{adj} , RMSE, and SSE, the Redlich–Peterson (R–P) model was among the best isotherm models for Cr(VI) adsorption

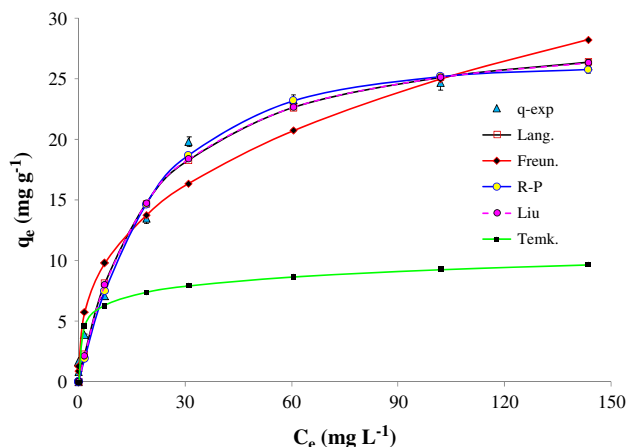


Fig. 9. Non-linear isotherm curves of Cr(VI) adsorption on ST/Mag (conditions: C_o 5–300 mg L⁻¹, pH 2.0, adsorbent dose 6 g L⁻¹, contact time 120 min, TDS 0.5%, and $T = 20 \pm 1$ °C).

by ST/Mag adsorbent, since g is more than 1, this isotherm model is invalid. The Temkin isotherm model was not suitably fitted Cr(VI) adsorption experimental data, presenting higher RMSE and SSE values. Therefore, the isotherm parameters of the Temkin model are not presented in Table 3. Regardless of the Redlich–Peterson (R–P) model, the best fit is obtained using the Langmuir and Liu models as well, although the fitting by Freundlich isotherm model is only slightly worse (see Fig. 9 and Table 3). The Langmuir model suggests a uniform distribution of homogeneous active sites on the adsorbent surface as well as a monolayer and homogeneous adsorption of Cr(VI) on ST/Mag nanoparticles. Moreover, as shown in Table 3, it is obvious that the obtained values of R_L dimensionless separation factor are less than one at all the studied concentrations, confirming favorable adsorption of Cr(VI) onto ST/Mag. Previous studies have also reported that the Langmuir isotherm is the best model for the experimental data of Cr(VI) adsorption on other magnetite-based adsorbents [3,25,45,51]. Table 3 presents a comparison of sorption capacities of Cr(VI) adsorbed in different magnetite-based adsorbents. The maximum amount of Cr(VI) uptake per unit mass of ST/Mag was 30.03 mg g⁻¹ based on the Langmuir equilibrium model. Despite the presence of high concentrations of salt (TDS 5,000 mg L⁻¹), as shown in Table 4, the ST/Mag adsorbent presented good sorption capacities compared to other magnetite-based adsorbents.

The most probable reason for the lower maximum adsorption capacity of ST/Mag in this study, compared to other adsorbents such as diatomite-supported magnetite [25] and MCCAC [52] is the presence of a high amount of anions and cations along with Cr(VI), which are competing to adsorb Cr(VI) by ST/Mag nanoparticles.

3.6. Effect of presence of co-ions on adsorption process

As Cr(VI) and co-ions usually coexist in industrial wastewater (e.g. tannery wastewater), Cr(VI) removal in the presence of co-ions seems to be necessary. Ionic strength is directly proportional to the ion concentration of aqueous solutions. Ionic strength is also one of the most important factors which influence the aqueous phase equilibrium. Generally, adsorption capacity decreases as a result of increasing the ionic strength of the aqueous solution due to the competitive adsorption of co-ions onto the adsorbent surface [47]. Table 5 shows the effect of co-ions on the uptake of Cr(VI) ($C_o = 10$ mg L⁻¹) on ST/Mag nanoparticles at pH 2 using 6 g L⁻¹ adsorbent mass. Obviously, there are insignificant decreases in Cr(VI) uptake by increasing

Table 3

Goodness of fit criteria and isotherm constants of different models for the adsorption of Cr(VI) onto ST/Mag (conditions: C_0 5–300 mg L⁻¹, pH 2.0, adsorbent dose 6 g L⁻¹, contact time 120 min, TDS 0.5%, and $T = 20 \pm 1$ °C)

Adsorption isotherm models	Parameters (unit)	Values	R ² adj	RMSE	SSE
Langmuir $q_e = \frac{K_L q_m C_e}{1 + K_L C_e}$	q_m (mg g ⁻¹)	30.03	0.987	1.20	11.43
	K_L (L mg ⁻¹)	0.0505			
	R_L	0.06–0.80			
Freundlich $q_e = K_F C_e^{\frac{1}{n}}$	K_F (mg g ⁻¹)(mg L ⁻¹) ⁻ⁿ	4.827	0.962	2.06	34.07
	n (-)	2.813			
	Redlich–Peterson $q_e = \frac{K_{RP} C_e}{1 + a_{RP} C_e^g}$	K_{RP} (L g ⁻¹)			
a_{RP} (L mg ⁻¹)	0.021				
g (-) ($0 < g < 1$)	1.131				
Liu $q_e = \frac{q_m (K_g C_e)^{n_L}}{1 + (K_g C_e)^{n_L}}$	q_m (mg g ⁻¹)	29.64	0.986	1.28	11.39
	K_g (L mg ⁻¹)	0.052			
	n_L (-)	1.032			

Table 4

The adsorptive capacities of various magnetite-based adsorbents for Cr(VI)

Adsorbent	q_m (mg g ⁻¹)	pH	References
MagMt ^a	15.3	2–2.5	[45]
Magnetite	10.6	2–2.5	[45]
Magnetite–maghemite	2.4	2.0	[47]
SLS-modified magnetite	30.7	4.0	[4]
Diatomite-supported magnetite	69.2	2–2.5	[25]
Magnetite nanoparticle	21.7	2–2.5	[25]
Magnetite-PEI800-MMT	8.8	1–9	[51]
MCCAC ^b	57.4	2.0	[52]
ST/Mag nanoparticle	30.0	2.0	This study

^aMontmorillonite-supported magnetite.

^bActivated carbon prepared from corn cob biomass, magnetized by magnetite nanoparticles.

co-ions from 0.05 to 0.5%. Additionally, increasing the concentration of co-ions from 0.5 to 5.0%, decreased Cr(VI) adsorption efficiency and q_m as much as only 21%. This slight decrease in removal percentages and maximum capacities occurring in the presence of salt ions may be attributed to the inhibition effect of salt on the adsorption of Cr(VI) ions onto adsorbent

Table 5

Data obtained for the adsorption of chromium (10 mg L⁻¹) from different solutions using ST/Mag nanoparticles (6.0 g L⁻¹) (pH 2, contact time = 60 min, and $T = 20 \pm 1$ °C)

Concentration of co-ions (%)	ST/Mag	
	Removal (%)	q_m (mg g ⁻¹)
0.05	99.9 (±0.04)	1.39 (±0.00)
0.5	99.7 (±0.15)	1.39 (±0.00)
5.0	78.3 (±1.92)	1.09 (±0.03)

surface and or the relative competition between salt ions (Cl⁻, SO₄²⁻, etc.) and chromate anions on the available active sites of ST/Mag. Some inorganic ions, such as chloride, may form complexes with some metal ions and therefore affect the adsorption process [53]. The results indicate that ST/Mag nanoparticles can remove such low concentrations of Cr(VI) in the presence of co-ions. The reason was that the two components of ST/Mag, i.e. spent tea and magnetite, dominated the sorption of Cr(VI) and co-ions simultaneously. The results suggested that ST/Mag nanoparticles can be used as a sorbent to remove Cr (VI) from saline wastewater.

3.7. Desorption studies and reusability

Desorption studies will help to recover Cr(VI) from sorbent. Moreover, these studies will not only help to regenerate the sorbents so that they can be reused to

adsorb metal ions, but can also help to develop successful sorption processes [54]. The desorption ratio of Cr(VI) from adsorbent can be calculated using Eq. (4) as follows:

$$\%DR = \frac{C_{des}}{C_{ads}} \times 100 \quad (4)$$

where % DR is the desorption ratio, C_{ads} is the amount of Cr(VI) sorbed onto the adsorbent, and C_{des} is the amount of Cr(VI) desorbed from the adsorbent.

Desorption experiments were carried out with 50-ml Cr(VI) solutions (initial Cr(VI) concentration 10 mg L^{-1} , co-ion concentration 0.5%, room temperature $20 \pm 1^\circ\text{C}$, contact time 60 min, and 6 g L^{-1} ST/Mag nanoparticles) using 0.2 M NaOH and 0.2 M NaOH + 1.0 M NaCl [55–57]. Activation of ST/Mag nanoparticles after the desorption process was achieved by agitation with 1.0 M HCl for 120 min followed by washing with distilled water. Accordingly, as shown in Table 6, the process of sorption/desorption was repeated for five successive cycles and the adsorbent showed slight decrease (about 10%) in the uptake capacity during successive cycles. On the whole, the desorption ratio of Cr(VI) using 0.2 M NaOH and 0.2 M NaOH + 1.0 M NaCl was over 87.2 (± 3.8)% and 93.2 (± 2.9)%, respectively (Table 6). However, the desorption ratio of Cr(VI) decreased, but the adsorption capacity of the ST/Mag nanoparticles could still be maintained at 90% level at the fifth cycle, as shown in Table 6. Other studies have also reported high elution efficiency of Cr(VI) using alkaline eluents [55,57]. These results indicate no significant loss in the activity of ST/Mag nanoparticles over at least five cycles of adsorption/desorption, which reveals the potential reusability of ST/Mag nanoparticles for the removal of metal ions from saline wastewater.

Table 6

Repeated adsorption of Cr(VI) ions using ST/Mag nanoparticles (initial concentration 10 mg L^{-1} , ST/Mag 6.0 g L^{-1} , pH 2.0, contact time 60 min, and $T = 20 \pm 1^\circ\text{C}$)

Cycle number	Desorption ratio (%)	
	NaOH	NaCl + NaOH
1	91.9 (± 1.5)	97.3 (± 0.5)
2	90.0 (± 0.6)	95.4 (± 0.4)
3	87.4 (± 0.5)	92.5 (± 1.0)
4	85.3 (± 0.3)	91.0 (± 0.6)
5	81.6 (± 0.9)	90.0 (± 0.6)
Mean	87.2 (± 3.8)	93.2 (± 2.9)

4. Conclusion

The (ST/Mag) nanoparticles were prepared, characterized, and used successfully in batch adsorption experiments for Cr(VI) uptake from saline aqueous media. The adsorption process was found to be pH dependent with the optimal pH of 2.0. The kinetics study of Cr(VI) adsorption onto ST/Mag using different general kinetic models was also examined. The sorption seems to be governed by chemical forces rather than physical electrostatic interactions, best described by the Avrami fractional-order and the pseudo-second-order kinetic models in which the rate-limiting step is assumed to be the chemical sorption between the adsorbate and the adsorbent. Furthermore, the equilibrium data could best be described by the Langmuir and Liu isotherm models with a monolayer sorption capacity of 30.0 mg g^{-1} . The presence of co-ions showed an insignificant effect on the uptake of Cr(VI) ions. Desorption of Cr(VI) ions and feasible recovery of ST/Mag were achieved using alkaline eluents with efficiencies of greater than 90%. The results clearly confirm that ST/Mag nanoparticles easily synthesized as a cost-effective, environmental friendly, and robust adsorbent and can be successfully used to remediate saline wastewater containing heavy metal ions.

Supplementary material

The supplementary material for this paper is available online at <http://dx.doi.org/10.1080/19443994.2015.1052990>.

Acknowledgements

This paper is issued from thesis of Zeynab Baboli. The financial support of the Vice-Chancellor for Research Affairs of Ahvaz Jundishapur University of Medical Sciences, grant No: ETRC9105, is gratefully acknowledged.

References

- [1] Â.L. Andrade, D.M. Souza, M.C. Pereira, J.D. Fabris, R.Z. Domingues, pH effect on the synthesis of magnetite nanoparticles by the chemical reduction-precipitation method, *Quim. Nova* 33 (2010) 524–527.
- [2] M.M. Amin, A. Khodabakhshi, M. Mozafari, B. Bina, S. Kheiri, Removal of Cr(VI) from simulated electroplating wastewater by magnetite nanoparticles, *Environ. Eng. Manage. J.* 9 (2010) 921–927.
- [3] N. Ballav, H.J. Choi, S.B. Mishra, A. Maity, Synthesis, characterization of Fe₃O₄@glycine doped polypyrrole magnetic nanocomposites and their potential performance to remove toxic Cr(VI), *J. Ind. Eng. Chem.* 20 (2014) 4085–4093.

- [4] A.A. Babaei, Z. Baboli, N. Jaafarzadeh, G. Goudarzi, M. Bahrami, M. Ahmadi, Synthesis, performance, and nonlinear modeling of modified nano-sized magnetite for removal of Cr(VI) from aqueous solutions, *Desalin. Water Treat.* 53 (2015) 768–777.
- [5] P. Yuan, M. Fan, D. Yang, H. He, D. Liu, A. Yuan, J. Zhu, T. Chen, Montmorillonite-supported magnetite nanoparticles for the removal of hexavalent chromium [Cr(VI)] from aqueous solutions, *J. Hazard. Mater.* 166 (2009) 821–829.
- [6] A. Zhu, L. Yuan, T. Liao, Suspension of Fe₃O₄ nanoparticles stabilized by chitosan and o-carboxymethylchitosan, *Int. J. Pharm.* 350 (2008) 361–368.
- [7] M. Bahrami, S. Boroomandnasab, H.A. Kashkuli, A. Farrokhan Firouzi, A.A. Babaei, Removal of Cd(II) from aqueous solution using modified Fe₃O₄ nanoparticles, *Rep. Opin.* 4 (2012) 31–40.
- [8] A.A. Babaei, M. Bahrami, A. Farrokhan Firouzi, A. Ramazanpour Esfahani, L. Alidokht, Adsorption of cadmium onto modified nanosized magnetite: Kinetic modeling, isotherm studies, and process optimization, *Desalin. Water Treat.* (2014) 1–13, doi:10.1080/19443994.2014.972986.
- [9] A. Novakova, V.Y. Lanchinskaya, A. Volkov, T. Gendler, T.Y. Kiseleva, M. Moskvina, S. Zezin, Magnetic properties of polymer nanocomposites containing iron oxide nanoparticles, *J. Magn. Magn. Mater.* 258–259 (2003) 354–357.
- [10] A. Ramazanpour Esfahani, A. Farrokhan Firouzi, G. Sayyad, A. Kiasat, Isotherm study of cadmium adsorption onto stabilized-zerovalent iron nanoparticles, *Int. J. Agron. Plant Prod.* 4 (2013) 3444–3454.
- [11] A. Esfahani, A. Firouzi, G. Sayyad, A. Kiasat, L. Alidokht, A.R. Khataee, Pb(II) removal from aqueous solution by polyacrylic acid stabilized zero-valent iron nanoparticles: Process optimization using response surface methodology, *Res. Chem. Intermed.* 40 (2014) 431–445.
- [12] P. Yuan, M. Fan, D. Yang, H. He, D. Liu, A. Yuan, J. Zhu, T. Chen, Montmorillonite-supported magnetite nanoparticles for the removal of hexavalent chromium [Cr(VI)] from aqueous solutions, *J. Hazard. Mater.* 166 (2009) 821–829.
- [13] P. Yuan, D. Liu, M. Fan, D. Yang, R. Zhu, F. Ge, J. Zhu, H. He, Removal of hexavalent chromium [Cr(VI)] from aqueous solutions by the diatomite-supported/unsupported magnetite nanoparticles, *J. Hazard. Mater.* 173 (2010) 614–621.
- [14] S. Si, A. Kotal, T.K. Mandal, S. Giri, H. Nakamura, T. Kohara, Size-controlled synthesis of magnetite nanoparticles in the presence of polyelectrolytes, *Chem. Mater.* 16 (2004) 3489–3496.
- [15] I.J. Bruce, J. Taylor, M. Todd, M.J. Davies, E. Borioni, C. Sangregorio, T. Sen, Synthesis, characterisation and application of silica-magnetite nanocomposites, *J. Magn. Mater.* 284 (2004) 145–160.
- [16] A. Esfahani, S. Hojati, A. Azimi, L. Alidokht, A. Khataee, M. Farzadian, Reductive removal of hexavalent chromium from aqueous solution using sepiolite-stabilized zero-valent iron nanoparticles: Process optimization and kinetic studies, *Korean J. Chem. Eng.* 31 (2014) 630–638.
- [17] M. Arruebo, R. Fernández-Pacheco, S. Irusta, J. Arbiol, M.R. Ibarra, J. Santamaría, Sustained release of doxorubicin from zeolite-magnetite nanocomposites prepared by mechanical activation, *Nanotechnology* 17 (2006) 4057–4064.
- [18] M. Giahi, R. Rakhshae, M.A. Bagherinia, Removal of methylene blue by tea wastages from the synthesis waste waters, *Chin. Chem. Lett.* 22 (2011) 225–228.
- [19] T. Madrakian, A. Afkhami, M. Ahmadi, Adsorption and kinetic studies of seven different organic dyes onto magnetite nanoparticles loaded tea waste and removal of them from wastewater samples, *Spectrochim. Acta, Part A* 99 (2012) 102–109.
- [20] E. Malkoc, Y. Nuhoglu, Removal of Ni(II) ions from aqueous solutions using waste of tea factory: Adsorption on a fixed-bed column, *J. Hazard. Mater.* 135 (2006) 328–336.
- [21] B.M.W.P.K. Amarasinghe, R.A. Williams, Tea waste as a low cost adsorbent for the removal of Cu and Pb from wastewater, *Chem. Eng. J.* 132 (2007) 299–309.
- [22] E. Malkoc, Y. Nuhoglu, Potential of tea factory waste for chromium(VI) removal from aqueous solutions: Thermodynamic and kinetic studies, *Sep. Purif. Technol.* 54 (2007) 291–298.
- [23] M.K. Mondal, Removal of Pb(II) ions from aqueous solution using activated tea waste: Adsorption on a fixed-bed column, *J. Environ. Manage.* 90 (2009) 3266–3271.
- [24] P. Panneerselvam, N. Morad, K.A. Tan, Magnetic nanoparticle (Fe₃O₄) impregnated onto tea waste for the removal of nickel(II) from aqueous solution, *J. Hazard. Mater.* 186 (2011) 160–168.
- [25] P. Yuan, D. Liu, M. Fan, D. Yang, R. Zhu, F. Ge, J. Zhu, H. He, Removal of hexavalent chromium [Cr(VI)] from aqueous solutions by the diatomite-supported/unsupported magnetite nanoparticles, *J. Hazard. Mater.* 173 (2010) 614–621.
- [26] M. Ozmen, K. Can, G. Arslan, A. Tor, Y. Cengeloglu, M. Ersoz, Adsorption of Cu(II) from aqueous solution by using modified Fe₃O₄ magnetic nanoparticles, *Desalination* 254 (2010) 162–169.
- [27] G. Durai, M. Rajasimman, Biological treatment of tannery wastewater—A review, *J. Environ. Sci. Technol.* 4 (2011) 1–17.
- [28] K. Nagashanmugam, K. Srinivasan, Removal of chromium(VI) from aqueous solution by chemically modified gingelly oil cake carbon, *Indian J. Chem. Technol.* 18 (2011) 207–219.
- [29] M. Jain, V.K. Garg, K. Kadirvelu, Adsorption of hexavalent chromium from aqueous medium onto carbonaceous adsorbents prepared from waste biomass, *J. Environ. Manage.* 91 (2010) 949–957.
- [30] H. Li, S. Bi, L. Liu, W. Dong, X. Wang, Separation and accumulation of Cu(II), Zn(II) and Cr(VI) from aqueous solution by magnetic chitosan modified with diethylenetriamine, *Desalination* 278 (2011) 397–404.
- [31] American Society for Testing and Material (ASTM), Method D4749, Philadelphia, PA, 1994.
- [32] A. Ofomaja, E. Naidoo, Biosorption of lead(II) onto pine cone powder: Studies on biosorption performance and process design to minimize biosorbent mass, *Carbohydr. Polym.* 82 (2010) 1031–1042.
- [33] Y. Sharma, V. Srivastava, C. Weng, S. Upadhyay, Removal of Cr(VI) from wastewater by adsorption on iron nanoparticles, *Can. J. Chem. Eng.* 87 (2009) 921–929.

- [34] Annual book of ASTM standards test methods for chromium in water ASTM, American Society for Testing and Material (ASTM), Philadelphia, PA, 2002.
- [35] S. Zakhama, H. Dhaouadi, F. M'Henni, Nonlinear modelisation of heavy metal removal from aqueous solution using *Ulva lactuca* algae, *Bioresour. Technol.* 102 (2011) 786–796.
- [36] S. Rangabhashiyam, N. Anu, M.S. Giri Nandagopal, N. Selvaraju, Relevance of isotherm models in biosorption of pollutants by agricultural byproducts, *J. Environ. Chem. Eng.* 2 (2014) 398–414.
- [37] S. Lagergren, About the theory of so-called adsorption of soluble substances, *Kungliga Svenska Vetenskapsakademiens Handlingar*, 24(4) (1898) 1–39.
- [38] Y.S. Ho, G. McKay, Pseudo-second order model for sorption processes, *Process Biochem.* 34 (1999) 451–465.
- [39] S. Senthilkumar, P. Varadarajan, K. Porkodi, C. Subbhuraam, Adsorption of methylene blue onto jute fiber carbon: Kinetics and equilibrium studies, *J. Colloid Interface Sci.* 284 (2005) 78–82.
- [40] M. Kapoor, P. Srivastava, I. Kapoor, G. Singh, R. Fröhlich, X-ray crystallography and thermolysis of halide salts of 2, 4, 6-trimethylaniline, Part: 90, *Energy Environ. Focus* 2 (2013) 46–50.
- [41] M.A. Hossain, H.H. Ngo, W.S. Guo, T. Setiadi, Adsorption and desorption of copper(II) ions onto garden grass, *Bioresour. Technol.* 121 (2012) 386–395.
- [42] K.Y. Foo, B.H. Hameed, Insights into the modeling of adsorption isotherm systems, *Chem. Eng. J.* 156 (2010) 2–10.
- [43] D.L. Pavia, G.M. Lampman, G.S. Kriz, J.R. Vyvyan, *Introduction to Spectroscopy*, fourth ed., Cengage Learning, Boston, MA, 2008.
- [44] V. Gopalakannan, N. Viswanathan, Synthesis of magnetic alginate hybrid beads for efficient chromium (VI) removal, *Int. J. Biol. Macromol.* 72 (2015) 862–867.
- [45] P. Yuan, M. Fan, D. Yang, H. He, D. Liu, A. Yuan, J. Zhu, T. Chen, Montmorillonite-supported magnetite nanoparticles for the removal of hexavalent chromium [Cr(VI)] from aqueous solutions, *J. Hazard. Mater.* 166 (2009) 821–829.
- [46] J. Yang, M. Yu, W. Chen, Adsorption of hexavalent chromium from aqueous solution by activated carbon prepared from longan seed: Kinetics, equilibrium and thermodynamics, *J. Ind. Eng. Chem.* 21 (2015) 414–422.
- [47] S.R. Chowdhury, E.K. Yanful, Arsenic and chromium removal by mixed magnetite–maghemite nanoparticles and the effect of phosphate on removal, *J. Environ. Manage.* 91 (2010) 2238–2247.
- [48] I. Khazaei, M. Aliabadi, H.T. Mosavian, Use of agricultural waste for removal of Cr(VI) from aqueous solution, *Iran. J. Chem. Eng.* 8 (2011) 11–23.
- [49] Y. Jung, J. Choi, W. Lee, Spectroscopic investigation of magnetite surface for the reduction of hexavalent chromium, *Chemosphere* 68 (2007) 1968–1975.
- [50] X.S. Wang, Y.J. Tang, L.F. Chen, F.Y. Li, W.Y. Wan, Y.B. Tan, Removal of Cr(VI) by zero valent, iron encapsulated alginate beads, *CLEAN–Soil, Air, Water* 38 (2010) 263–267.
- [51] I. Larraza, M. López-González, T. Corrales, G. Marcelo, Hybrid materials: Magnetite–Polyethyleneimine–Montmorillonite, as magnetic adsorbents for Cr(VI) water treatment, *J. Colloid Interface Sci.* 385 (2012) 24–33.
- [52] S. Nethaji, A. Sivasamy, A.B. Mandal, Preparation and characterization of corn cob activated carbon coated with nano-sized magnetite particles for the removal of Cr(VI), *Bioresour. Technol.* 134 (2013) 94–100.
- [53] G. Dönmez, Z. Aksu, Removal of chromium(VI) from saline wastewaters by *Dunaliella* species, *Process Biochem.* 38 (2002) 751–762.
- [54] A. Nemr, Potential of pomegranate husk carbon for Cr(VI) removal from wastewater: Kinetic and isotherm studies, *J. Hazard. Mater.* 161 (2009) 132–141.
- [55] Y.G. Abou El-Reash, M. Otto, I.M. Kenawy, A.M. Ouf, Adsorption of Cr(VI) and As(V) ions by modified magnetic chitosan chelating resin, *Int. J. Biol. Macromol.* 49 (2011) 513–522.
- [56] A.E. Nemr, Potential of pomegranate husk carbon for Cr(VI) removal from wastewater: Kinetic and isotherm studies, *J. Hazard. Mater.* 161 (2009) 132–141.
- [57] K.Z. Elwakeel, Removal of Cr(VI) from alkaline aqueous solutions using chemically modified magnetic chitosan resins, *Desalination* 250 (2010) 105–112.